PROBABLE MECHANISM OF CRACKING OF STABLE-AUSTENITIC WELDS CAUSED BY OXYGEN SEGREGATION

K.A. YUSHCHENKO, V.S. SAVCHENKO, N.O. CHERVYAKOV and **A.V. ZVYAGINTSEVA**
E.O. Paton Electric Welding Institute, NASU, Kiev, Ukraine

Current concepts of the nature of formation of cracks classified as ductility-dip cracks in multilayer welds or HAZ of steels and alloys with single-phase structure have been reviewed. It is noted that the mechanism of formation of such cracks is a subject of discussion. A hypothesis of the probable influence of oxygen on the processes of intergranular fracture is set forth, as oxygen decreases cohesion strength of grain boundaries in the established temperature range and leads to intergranular fracture.

Keywords: *arc welding, high-alloy steels, nickel alloys, welded joints, grain boundaries, ductility-dip cracks, cohesion energy, Auger-spectroscopy*

Welded joints on high-alloy steels with stable-austenitic structure and nickel superalloys are known to be highly sensitive to hot cracking during fusion welding. As to their nature, hot cracks are of two types: solidification and underbead (ductility-dip) cracks formed under thermal-force loading of the zones of metal of the multilayer welds (Figure 1). The temperature range of formation of solidification cracks (brittle temperature range — BTR) depends upon the range of the solid-liquid state of metal in solidification of the weld. The lower limit of this range is determined by the value of solidus temperature T_s at the end of solidification. The ductility-dip crack (DDC) temperature range is determined by an approximate ratio of $(0.6-0.8)T_s$ (Figure 1). The cracks in this range initiate and propagate along the boundaries of high-angle austenitic grains (Figure 2).

Some researchers relate the mechanism of ductility-dip cracking to embrittlement of grain boundaries, resulting from formation of a chain of precipitated carbides $Me_{23}C_6$ [2–4]. Investigations were conducted on nickel alloy Inconel 52. According to the suggested mechanism, metal carbides (of the $Me_{23}C_6$ type) precipitating along the grain boundaries (Figure 3) act as stress raisers that cause microstrains, thus promoting initiation of discontinuities and, as a consequence, grain boundary fracture. By accepting this mechanism of formation of cracks, it can be assumed that the intergranular fracture surface should have a pit-like (cup-shaped) character of fracture, at which the majority of pits comprise a carbide particle. This mechanism is characteristic of a tough intergranular fracture of high-alloy steel with a stable-austenitic structure at room temperature (Figure 4).

At the same time, examinations of the fracture surface in the zones of formation of DDCs [5] do not confirm occurrence of this mechanism. The authors of study [5] note formation of a wavy fracture surface in plane of grains, which are sometimes decorated with carbides. The sites of carbides are free from local plastic strains that form characteristic zones with the pit-like fracture mechanism (Figure 5). Analysis of the majority of results of fractographic examinations of the fracture surfaces shows [5] that carbides could not participate in formation of cracks within the ductility-dip range. Hence, the probability exists of occur-

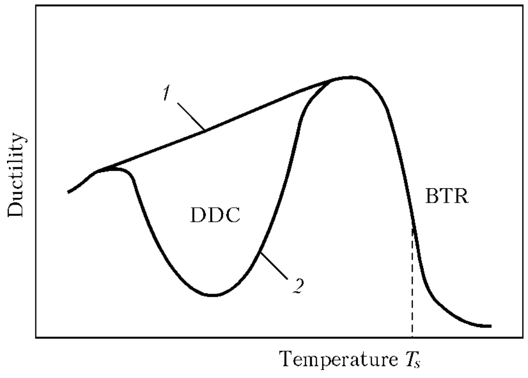

Figure 1. Diagram of formation of hot cracks in welded joints on high-alloy steels and alloys [1]: *1* — material without ductility dip; *2* — with ductility dip

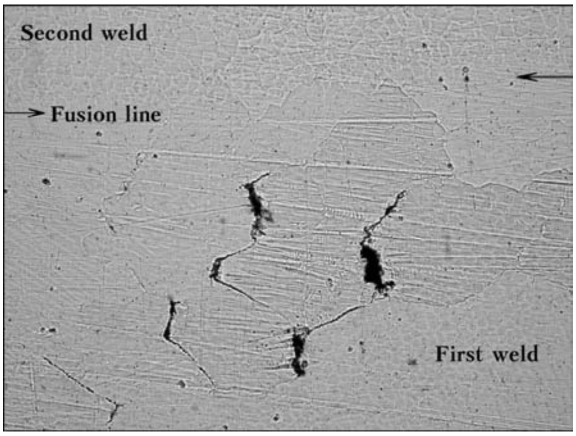

Figure 2. Microstructure (×200) of metal of the beads deposited with wire In52 with DDCs in multilayer welds

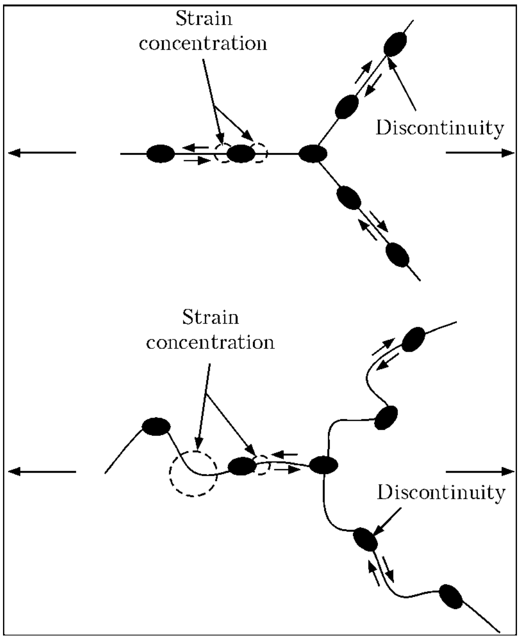

Figure 3. Effect of intergranular precipitates in formation of DDCs for straight and wavy grain boundaries [4]

rence of the fracture mechanism other than that put forth by the authors of the hypothesis described in studies [2–4]. Another confirmation of invalidity of the carbide theory are the results of evaluation of sensitivity to ductility-dip cracking using a high-alloy steel of the AISI 310 type (Table) with a different content of impurities [6].

Analysis of the published results of study [6] shows that steel SUS 310EHP, which is super pure in terms of the content of impurities, is insensitive to solidification cracks (Figure 6). Nevertheless, the authors note the presence of DDCs (DDC zone) in the weld metal, despite the super low content of impurities, including carbon, this excluding formation of carbides along the grain boundaries. Therefore, it can be concluded that formation of DDCs in TIG welding is not controlled by precipitation of carbides along the high-angle austenite grain boundaries.

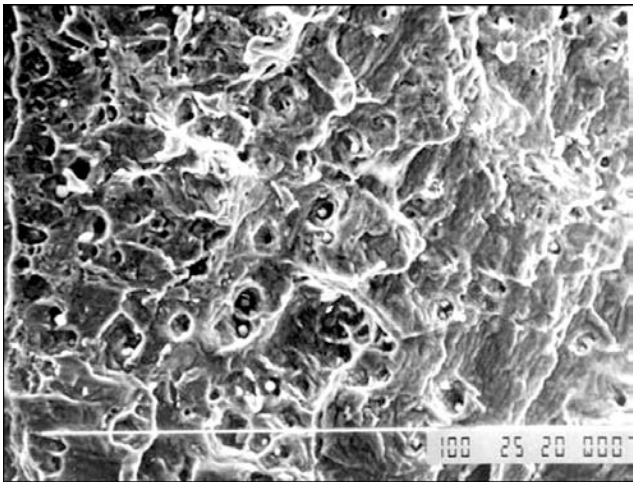

Figure 4. Fractogram of fracture surface on stable-austenitic weld metal with pit-like fracture character

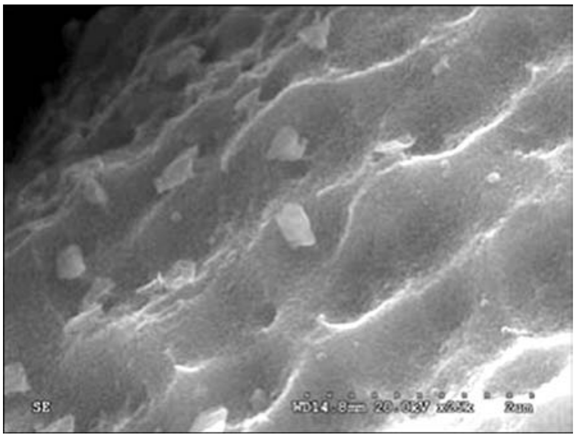

Figure 5. Fractogram of surface of DDCs with characteristic structure identified as wavy and decorated with carbide precipitates [5]

Analysis of chemical composition of super pure steel SUS 310EHP (see the Table) indicates that, along with such impurity elements as carbon, silicon, manganese, phosphorus and sulphur, the super pure metal also contains oxygen, its content being an order of magnitude higher than the content of carbon.

Consider the possible effect of oxygen on the processes of DDC formation. As shown earlier, the probable mechanism of DDC formation is enrichment of grain boundaries with impurity elements, which segregate to the boundaries in a temperature range of about $(0.6–0.8)T_s$ owing to the diffusion processes accelerated by plastic strains during welding [7].

Based on these conclusions, oxygen may affect the processes of intergranular embrittlement only in the case where this very active element exists in metal in a dissolved state and has a comparatively high diffusion coefficient in the fcc lattice. These data can be obtained by using the method of electromotive forces of metals in solid electrolytes with oxygen conductivity. The method is employed to determine parameters of diffusion of oxygen in solid solution of metallic

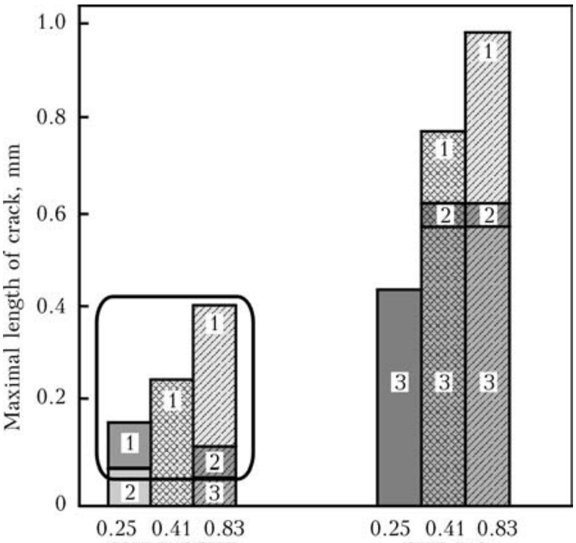

Figure 6. Maximal length of DDCs (*1*), transition zone (*2*) and solidification cracks (*3*) in stainless steels of the 310 type at strains of 0.25, 0.41 and 0.83 % [6]

Chemical composition of high-alloy steel SUS 310 [7] compared with super pure steel SUS 310EHP, wt.%

Steel grade (AISI 310 type)	C	Si	Mn	P	S	Ni	Cr	O	N	Ti	Fe
SUS 310EHP	0.0002	0.0025	0.0001	0.0011	0.0008	21.58	21.13	0.0029	0.0022	0.18	Base
SUS 310	0.12	1.00	1.48	0.020	0.011	20.59	25.12	–	–	–	Same

materials, including with the fcc lattice [8, 9]. In this case, a solid electrolyte consisting of zirconia (85 %) with additions of Y_2O_3 (15 %) is used as an ion conductor.

The above electrochemical method allows using ZrO_2 as a practically pure ion conductor to investigate diffusion of oxygen in solid metals at high temperatures. In this case, the diffusion flow of oxygen transforms into the electric current, the value of which can be measured.

Qualitative investigations conducted by the authors using the solid electrolyte on high-alloy steel EI417 (Kh23N18) (GOST 5632–72) showed the presence of current in an electric circuit, this being indicative of the diffusion of oxygen in the crystalline lattice.

The published data on the quantitative proportion of oxygen show that in a structural steel that is not deoxidised by aluminium the total content of oxygen is 105 ppm, and that of diffusible oxygen is 40 ppm [10]. In deoxidation, the total and diffusible oxygen contents decrease accordingly.

The rate of diffusion of oxygen in iron with γ-structure at high temperatures is shown in Figure 7.

Analysis of the presented data allows compiling a series of diffusion mobility of hydrogen, oxygen, carbon, nitrogen and sulphur depending upon the temperature, the diffusion coefficient of oxygen being more than two orders of magnitude higher than that of sulphur.

Therefore, there are preconditions for diffusion redistribution of oxygen between the grain body and boundary, which is likely to be accelerated by dislocation transfer of impurity elements at plastic strains under the effect of a welding thermal cycle.

It can be assumed on the basis of these data that in the SUS 310EHP metal, which is super pure in terms of sulphur, carbon and phosphorus, the element that leads to the DDC formation [7] is oxygen. It should be taken into account in this case that the source of ingress of oxygen into the weld pool and weld (by an example of TIG welding) is not only oxygen contained in the base and filler metal, but also the always existing probability of saturation of the weld pool with oxygen in argon welding.

The model of intergranular fracture in formation of DDCs can be represented by a diagram shown in Figure 8. According to this diagram, strength of interatomic bonds is determined by attractive and repulsive forces between the elementary particles that are in the equilibrium state and determine the energy of cohesion of atoms at the grain boundaries.

The process of segregation of some elements, including oxygen, in the field of stresses at the boundary crack apex (Figure 9) leads to a change in the cohesion strength, thus favouring redistribution of the atomic interaction forces and sensitivity to intergranular embrittlement as a whole (Figure 10).

The latter follows both from general considerations of the effect of segregations on the cohesion strength of interfaces, and from estimations of the strength by the formula in studies [14, 15], derived from an upgraded model of allowance for the role of segregations:

$$\sigma_m^s = \frac{\sigma_m^0}{1 + 1/2X_i(a_1/a_0 - 1)},$$

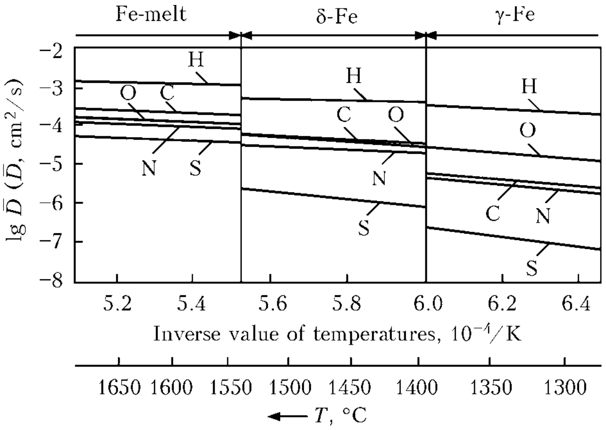

Figure 7. Temperature dependence of mean value of diffusion coefficient for elements in iron [11]

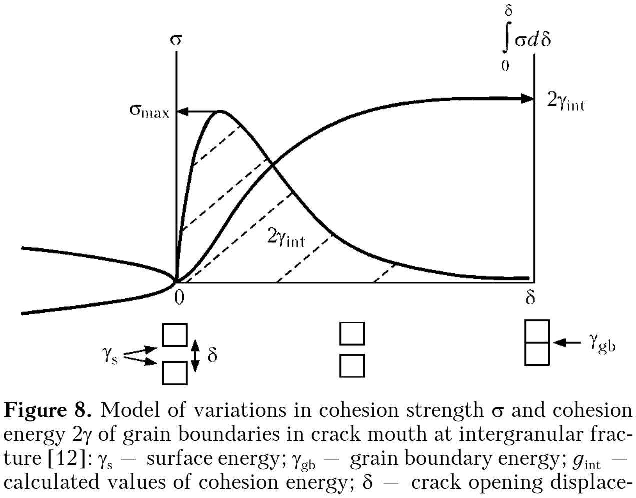

Figure 8. Model of variations in cohesion strength σ and cohesion energy 2γ of grain boundaries in crack mouth at intergranular fracture [12]: γ_s — surface energy; γ_{gb} — grain boundary energy; g_{int} — calculated values of cohesion energy; δ — crack opening displacement

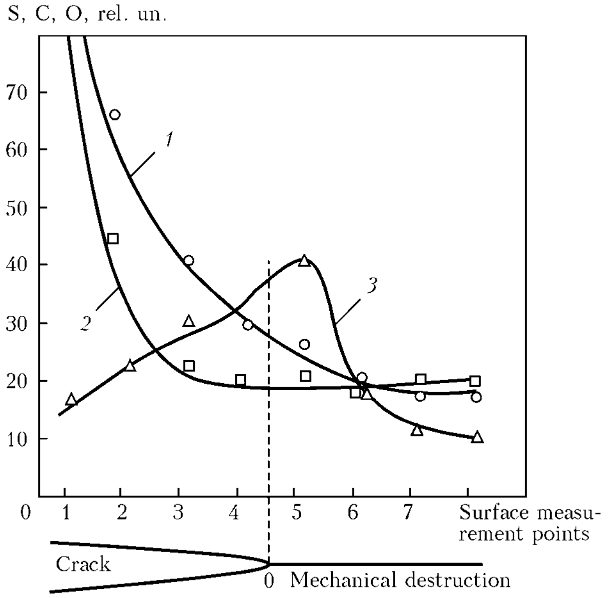

Figure 9. Character of distribution of impurity elements ahead of the crack apex at high-temperature fracture [13]: *1* — oxygen; *2* — carbon; *3* — sulphur

where σ_m^0 is the strength of cohesion of a clean interface; X_i is the concentration of a segregating element at the interface; a_1 and a_2 are the atomic sizes of the segregating atoms and matrix atoms, respectively.

Consider the probable effect of carbon and oxygen on the processes of variations in cohesion strength of interfaces, proceeding from sizes of the atomic radii of iron and nickel as a base of the majority of high-alloy steels and alloys with a stable-austenitic structure (values of the atomic radii of some elements [16] are as follows, nm: 0.1411 Fe, 0.1377 Ni, 0.1606 O, 0.1281 C) for oxygen — $(a_1/a_0 - 1) > 0$ $[-\sigma]$ and for carbon — $(a_1/a_0 - 1) < 0$ $[+\sigma]$ $2\gamma \rightarrow [-\sigma]$.

Considering the positive value of the $(a_1/a_0 - 1)$ ratio for oxygen, one may expect decrease in the values of interfacial cohesion strength in iron- and nickel-base materials and resistance to DDC formation as a whole caused by this element.

As shown by similar calculations, in contrast to oxygen, carbon gives a negative value of the above ratio. It does not decrease the interfacial cohesion strength of iron- and nickel-base materials. Thus, it does not lead to formation of DDCs in the investigated grades of materials in accordance with the accepted model.

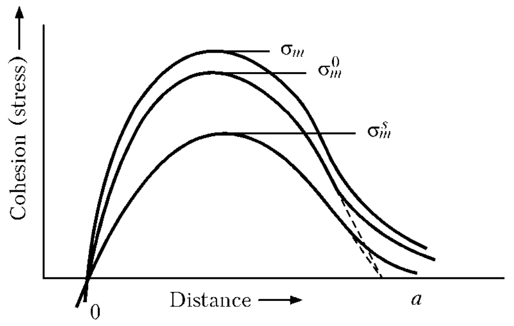

Figure 10. Variation in cohesion intergranular stress as a function of distance from the crack apex [14]: σ_m — cohesion energy of grain body; σ_m^0 — cohesion energy of clean boundary; σ_m^s — cohesion energy of boundary with an impurity; *a* — distance from the crack front in stress field

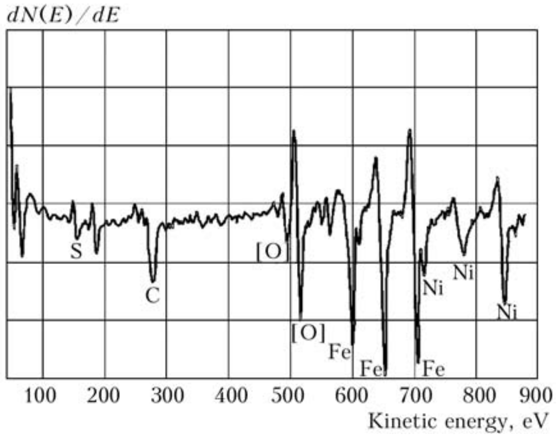

Figure 11. Energy spectrum of relative distribution of main alloying and impurity elements on the crack surface in weld metal of the 34NKD type metal

Along with the parameters of atoms and in accordance with the given formula, a decisive effect on the cohesion strength processes is exerted by the concentration of impurity elements along the grain boundaries as a result of their segregation.

The concentration of oxygen and carbon on the surface of brittle intergranular fracture was evaluated by Auger-spectroscopy on uniaxial tension specimens of iron-nickel alloy 34NKD stretched in a 10^{-5} mm Hg vacuum at a ductility dip temperature of 850 °C and strain rate of $2.85 \cdot 10^{-4}$ s^{-1}. The choice of the above material was based on the absence of chromium in it (in contrast to the majority of high-alloy steels and alloys with a stable-austenitic structure), whose peak in the Auger-spectroscope energy spectrum almost coincides with the oxygen peak, which does not allow separating contents of these elements.

Chemical composition of alloy 34NKD (according to TU 14-1-3798–84) used for the experiments is as follows, wt.%: ≤0.03 C, ≤0.10 Mn, ≤0.10 Si, ≤0.10 Ti, <0.008 P, <0.01 S, 34–35 Ni, 1.5–2.0 Co, 9.2–0.4 Cu.

The contents of carbon, oxygen and sulphur were estimated from the Auger-analysis data using the «Riber» instrument LAS-2000 at a depth of about 5 nm from the crack surface after its ion beam cleaning

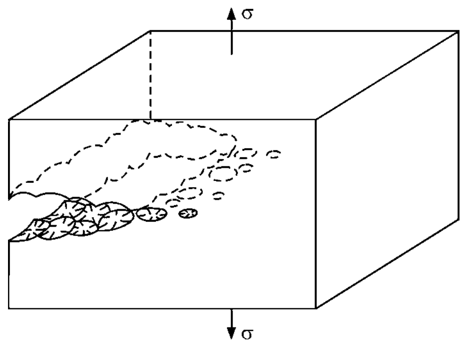

Figure 12. Model of formation of meniscus instability of material in formation of a wavy character of surface fracture [15]

from sorbates. The energy spectrum of a relative distribution of elements is shown in Figure 11.

The content of some elements on the intergranular fracture surfaces of the 34NKD alloy specimens was as follows, at.%: 29.3 C, 34.0 O and 1.2 S.

Analysis of the results indicates to enrichment of the surfaces of grain boundaries with oxygen, carbon and sulphur. Based on the values of the $(a_1/a_0 - 1)$ ratio, oxygen and sulphur may decrease the cohesion strength of grain boundaries. Carbon does not lead to decrease in the cohesion strength, as its $(a_1/a_0 - 1)$ ratio has a negative value, and the value of cohesion strength σ_m does not decrease (see the formula). Compared to sulphur, oxygen leads to a higher loss of the cohesion strength, proceeding from its increased content at the boundary. The increased oxygen content, compared with the sulphur content, can be attributed to high parameters of the diffusion coefficient of oxygen (see Figure 7).

Preliminary results make it possible to set forth the hypothesis of a probable mechanism of formation of cracks in the base and weld metals of welded joints on high-alloy steels within the ductility-dip temperature range. It is likely that formation of the embryo discontinuities of microscopic sizes (Figure 12) leads not only to the formation and localisation of micropores in plane of the grain boundary, but also to the super equilibrium and super critical concentration of an impurity element in them, this practically causing a micro brittle fracture along the grain boundaries with a minimal formation of the plastic strain zones.

CONCLUSIONS

1. Actively diffusing impurities, such as carbon, oxygen, hydrogen and phosphorus, which are dissolved in metal, are redistributed in cooling of metal under the stress and temperature gradient conditions between a solid solution and different defects of structure of dislocation clusters, twins, grain boundaries and inclusions. The activated process of formation and movement of dislocations in the DDC range leads to a super equilibrium enrichment of grain boundaries with impurities. The higher the diffusion coefficient and concentration of an element, other conditions being equal, the higher is the effect of decrease in strength, and the higher is the degree of localisation of tensile stresses and strains at the boundary.

2. It is not improbable that the centres of the eutectic origin liquid phase of molecular sizes may also be formed in this case, as there is a close relationship between the rate of diffusion of impurity elements, activation of the process under certain conditions of the thermal-deformation effect, quantity and location of micro- and macrocracks in austenitic metal along the grain boundaries, characteristics of fracture and concentration of impurity elements on the fractured planes with propagation of cracks, and high percentage of the impurities (carbon, oxygen, hydrogen, sulphur, phosphorus, etc.) fixed on the crack surface. It can be concluded at a high probability degree that fracture in the ductility-dip temperature range occurs by the cohesion mechanism, and it is reasonable to choose methods for elimination of these cracks on the basis of this mechanism.

1. Collins, M.G., Lippold, J.C. (2008) An investigation of ductility dip cracking in nickel-based filler materials. Pt 1. *Welding J.*, 82(**10**), 288–295.
2. Young, G.A., Capobianco, T.E., Penik, M.A. et al. (2008) The mechanism of ductility dip cracking in nickel-chromium alloy. *Ibid.*, 87(**2**), 31–43.
3. Capobianco, T.E., Hausou, M.E. (2005) Auger spectroscopy results from ductility dip cracks opened under ultra-high vacuum. In: *Proc. of Int. Conf. on Trends in Welding Research* (16–18 May, 2005, Callaway Giardens Resort, Pine Mountain, Georgia, USA), 767–772.
4. Lippold, J.C., Nissley, N.E. (2007) Further investigations of ductility dip cracking in high chromium, Ni-base filler metals. *Welding in the World*, **9**/**10**, 24–30.
5. Noecker, F.F., DuPont, J.N. (2009) Metallurgical investigation into ductility dip cracking in Ni-based alloys. Pt 2. *Welding J.*, **3**, 62–77.
6. Nishimoto, K., Saida, K., Kiuchi, K. et al. (2008) Hot cracking behaviour of high-purity type 310 stainless steels. Material joining process. *IIW Doc. IX-H-G98–08*.
7. Yushchenko, K., Savchenko, V. (2008) Classification and mechanisms of cracking in welding high-alloy steels and nickel alloys in brittle temperature ranges. In: *Hot cracking phenomena in welds II*. Berlin, Heidelberg: Springer, 95–114.
8. Pang, Y.-W., Altstetter, G.I. (1987) The diffusion and solubility of oxygen in solid nickel. *Metal. Transact. A*, (**7**), 43–50.
9. Rickert, H., Steiuer, R. (1966) Elektrochemische Messung der Sauerstoffdiffusion in Metallen bei hoeheren Temperaturen. *Zeitschrift fuer Physikalische Chemie*, 49(**3–5**), 127–137.
10. Pietscyhmann, G., Noky, D. (1988) Anwendung des Sauerstoffpotentials-messtechnick in der Stahlwerk Praxis. *Neue Huette*, **6**, 210–214.
11. Bester, H., Lange, K.W. (1972) Abschaetzung mittlerer Werte fuer die Diffusion von Kohlenstoff, Sauerstoff, Wasserstoff, Stickstoff und Schwefel in festem und fluessigem Eisen. *Archiv fuer das Eisenhuettenwesen*, **3**, 207–213.
12. Yamaguchi, W. (2008) First-principles calculations of the grain-boundary cohesive energy – embrittling or strengthening effect of solute segregation in a bcc FeΣ3(111) grain boundary. *J. Japan Inst. of Metals*, 72(**9**), 658.
13. Hippsley, S.A., Rauh, H., Bullongh, R. (1984) Stress-driver solute enrichment of crack-tips during low-ductility intergranular fracture of low-alloy steel. *Acta Metallurgica*, 32(**9**), 1381–1394.
14. Hondros, E.D., Seah, M.P. (1977) Segregation to interfaces. *Int. Metals Rev.*, **12**, 288–292.
15. Zhebynev, D.A., Ukolova, O.G., Gelman, A.A. et al. (1985) Study of chemical composition of diffusion zone in solid phase Ti–6 % Al–4 % V alloy joint. Method of scanning Auger spectroscopy. *Fizika i Khimiya Obrab. Materialov*, **6**, 108–114.
16. King, H.W. (1982) Atomic size parameters for the elements. *J. Phase Equilibria*, 2(**4**), 527.
17. Dico, P., Ocelik, V., Hajko, V. et al. (1987) Porusovanie pasok kovovych skiel pri monotonnom Tahovom zatazovani. *Kovove Materialy*, 25(**5**), 523–536.